www.nature.com/mtna

Optimization of Ultrasound-mediated Anti-angiogenic Cancer Gene Therapy

Hiroko Fujii[1], Pratiek Matkar[1], Christine Liao[1], Dmitriy Rudenko[1], Paul JH Lee[1], Michael A Kuliszewski[1], Gerald J Prud'homme[2] and Howard Leong-Poi[1]

Ultrasound-targeted microbubble destruction (UTMD) can be used to deliver silencing gene therapy to tumors. We hypothesized that UTMD would be effective in suppressing angiogenesis within tumors, and that modulation of the ultrasound pulsing intervals (PI) during UTMD would affect the magnitude of target knockdown. We performed UTMD of vascular endothelial growth factor receptor-2 (VEGFR2) short hairpin (sh)RNA plasmid in an heterotopic mammary adenocarcinoma model in rats, evaluating PIs of 2, 5, 10, and 20 seconds. We demonstrated that UTMD with a PI of 10 seconds resulted in the greatest knockdown of VEGFR2 by PCR, immunostaining, western blotting, smaller tumor volumes and perfused areas, and lower tumor microvascular blood volume (MBV) and flow by contrast-enhanced ultrasound (CEU) compared with UTMD-treated tumors at 2, 5, and 20 seconds, control tumors, tumors treated with intravenous shRNA plasmid and scrambled plasmid. CEU perfusion assessment using the therapeutic probe demonstrated that tumors were fully replenished with microbubbles within 10 seconds, but incompletely replenished at PI-2 and PI-5 seconds. In conclusion, for anti-VEGFR2 cancer gene therapy by UTMD, PI of 10 seconds results in higher target knockdown and a greater anti-angiogenic effect. Complete replenishment of tumor vasculature with silencing gene-bearing microbubbles in between destructive pulses of UTMD is required to maximize the efficacy of anti-angiogenic cancer gene therapy.

Introduction

Gene therapy has the potential to become an effective weapon to help fight chronic diseases such ischemic cardiovascular disease,[1] neurodegenerative conditions,[2] and cancer.[3,4] For cancer gene therapy, one of the most important advances has been the discovery of RNA interference (RNAi) technology that can regulate the expression of target genes.[5,6] Despite the potential of RNAi therapies in cancers, there remain important limitations that hinder their progress to clinical application, including suboptimal delivery techniques and off-target side effects.[5,7] The development of effective delivery techniques and the identification of appropriate gene target(s) are needed for cancer gene therapy to become a viable treatment for patients.

Targeted tissue transfection can be enhanced by ultrasound-mediated disruption of intravenously administered DNA-bearing microbubbles.[8] This non-invasive strategy of ultrasound-targeted microbubble destruction (UTMD) is unique among gene delivery techniques, being predominantly an intravascular method of delivery where transfection occurs primarily within the endothelial surface of vessels.[9,10] This can be advantageous, whereby endothelial transfection of stromal cell derived factor–1 using UTMD allows homing and vascular engraftment of intravenously administered endothelial progenitor cells for combined gene-cell therapy for angiogenesis in chronic ischemia.[11] This ability to selectively target DNA transfection to the vascular endothelium makes UTMD uniquely suited for pro-angiogenic gene transfer for therapeutic neovascularization.[9–12]

UTMD has begun to be evaluated for cancer gene therapy using *in vivo* tumor models, including delivery of the suicide gene herpes simplex virus thymidine kinase,[13–16] short antisense oligodeoxynucleotide targeting the human androgen receptor,[17] and gene therapy targeted against apoptotic targets.[18,19] Remarkably, very few studies have investigated antiangiogenic gene therapies using UTMD,[20,21] with no studies of intravenously administered genes and microbubbles. Given the predominant vascular transfection, UTMD would be an ideal technique for targeted anti-angiogenic gene therapy to tumor vasculature to suppress neovascularization.

Vascular endothelial growth factors (VEGFs) are known to facilitate angiogenesis through binding to various receptors. One key receptor, VEGFR2, has been shown to be involved in the signaling cascade responsible for endothelial cell proliferation and migration contributing to neovascularization. In our present study, we hypothesized that UTMD of intravenously administered cationic microbubbles bearing plasmid DNA encoding for VEGFR2 short hairpin (sh)RNA would result in targeted knockdown of VEGFR2 and lead to reduced neovascularization in a heterotopic topic mammary adenocarcinoma model in rats. We chose shRNA over siRNA due to its advantages of greater efficacy, easy incorporation into plasmids and lower degradation by nucleases.[22] Furthermore, we hypothesized that for gene delivery, pulsing intervals (PIs) that allow full replenishment of the tumor microvasculature during UTMD would result in maximal anti-angiogenic effect within tumors. Study animals were divided into seven groups: (i) control tumors—no treatment, (ii) intravenous shRNA plasmid, (iii) UTMD of scrambled DNA

[1]Division of Cardiology, Department of Medicine, Keenan Research Centre in the Li Ka Shing Knowledge Institute, St. Michael's Hospital, University of Toronto, Toronto, Ontario, Canada; [2]Department of Laboratory Medicine and Pathobiology, Keenan Research Centre in the Li Ka Shing Knowledge Institute, St. Michael's Hospital, University of Toronto, Toronto, Ontario, Canada. Correspondence: Howard Leong-Poi, 6–044 Queen Wing, St. Michael's Hospital, 30 Bond Street, Toronto, Ontario M5B 1W8, Canada. E-mail: leong-poih@smh.ca

sequence plasmid, (iv) UTMD using PI-2 seconds, (v) UTMD using PI-5 seconds, (vi) UTMD using PI-10 seconds, and (vii) UTMD using PI-20 seconds.

Results

Tumor size and volume
Heterotopic tumors underwent UTMD at day 10 after implantation. At day 17, tumor volume was lowest after UTMD of VEGFR2 shRNA plasmid at PI-5 seconds and PI-10 seconds, compared with other treatment groups (tumor volume [ml] at day 17 (**Figure 1a**). Data on percentage change in total tumor area by 2D contrast-enhanced ultrasound (CEU) imaging at day 17 (normalized to area at day 10) is shown in
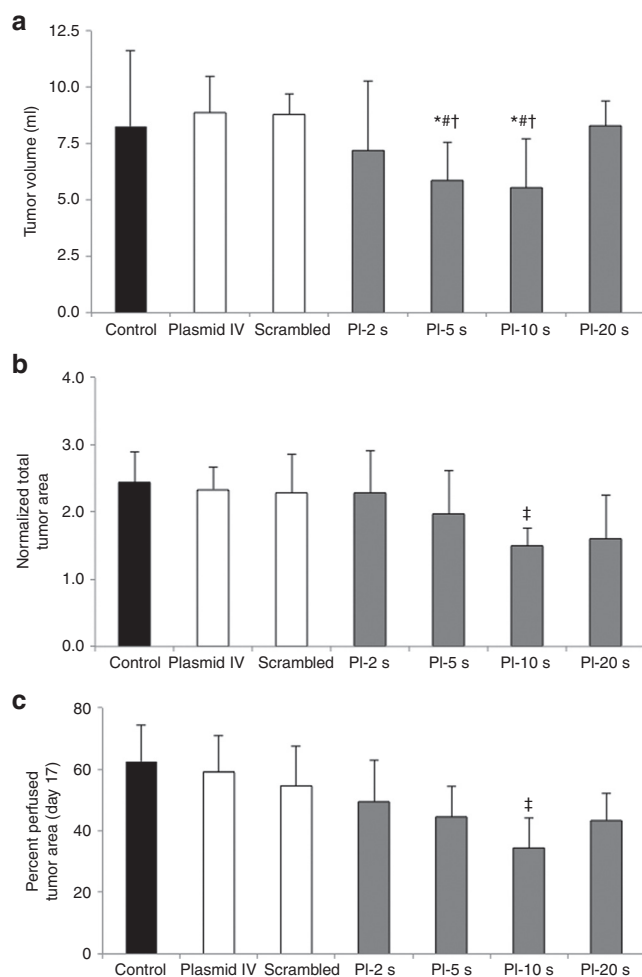
Figure 1 Tumor size assessment by volumetric displacement and ultrasound measurements (mean ± SD). (**a**) Tumor volume (ml) as measured by volumetric assessment, with smallest tumor volumes seen in the PI-5 seconds and PI-10 seconds groups. (**b**) Data on percent change in total tumor area (day 17/day 10) showing attenuated tumor growth in the PI-10 seconds group. (**c**) Data on percent perfused tumor area as measured by contrast-enhanced ultrasound perfusion imaging. As the PI during UTMD is increased, the percent of the tumor that is perfused becomes smaller, with the maximal reduction in tumor perfused area in the PI-10 seconds treatment group. *$P < 0.05$ versus control, #$P < 0.01$ versus plasmid IV and scrambled plasmid, †$P < 0.05$ versus PI-20 seconds, ‡$P < 0.05$ versus control, plasmid IV, and scrambled plasmid. PI, pulsing interval; UTMD, Ultrasound-targeted microbubble destruction.

Figure 1b. Similar to tumor volume, percent change in tumor area (day 17/day 10) was lowest in the PI-10 seconds group. Percent perfused tumor area (at plateau replenishment) at day 17 (the percent of the tumor area showing detectable perfusion by CEU) was smallest in the tumors treated with UTMD at PI-10 seconds, compared with the controls and the other PI groups (**Figure 1c**). As PI increases till 10 seconds during ultrasound-mediated anti-angiogenic gene delivery, percent perfused area within treated tumors decreases. Taken together, these results demonstrate that UTMD with PIs of 5 and 10 seconds are the most effective in suppressing tumor growth, with maximal reduction in both tumor volume and percent perfused area occurring when anti-angiogenic UTMD is performed at PI-10 seconds. At longer PIs of 20 seconds, efficacy is diminished likely due to the lower number (half those delivered with PI-10 seconds) of ultrasound pulses delivered during shRNA plasmid DNA circulation.

Perfusion imaging: contrast-enhanced ultrasound
Representative CEU perfusion images of tumors at day 10, before UTMD, and at day 17 from all treatment groups are shown in **Figure 2**. At day 10, there were no significant differences in microvascular blood volume (MBV) and microvascular blood flow between groups (**Figure 3a,c**). At day 17, the plateau signal intensity from tumors, representing MBV, was markedly reduced in the group treated with UTMD at PI-10 seconds as compared with scrambled plasmid, plasmid IV and control untreated animals (**Figure 3b**). Similar to MBV data, tumor microvascular blood flow was lower as PIs during UTMD was increased (up to PI-10 seconds), compared with control, plasmid IV, and scrambled shRNA plasmid groups (**Figure 3d**). UTMD of VEGFR2 shRNA plasmid DNA resulted in the greatest anti-angiogenic effect when delivered at the PI of 10 seconds.

When tumor perfusion was assessed at day 10 (pre-delivery) using the UTMD delivery probe (S3 transducer), quantitative analysis yielded a β value of 0.13 ± 0.04 seconds^{-1}. As β is the rate constant reflecting microbubble velocity within tumors, $1/\beta$ provides the time to plateau of full replenishment of the tumor microvasculature. Therefore, the average time for complete microbubble replenishment within day 10 tumors was 7.7 seconds. Thus, during UTMD, a PI-10 seconds allowed more complete replenishment of shRNA plasmid-bearing microbubbles in between destructive ultrasound pulses, and was less complete at shorter PIs of 2 and 5 seconds. Although PI-20 seconds also allows complete replenishment, the much longer PI resulted in significantly less destructive pulses (half those delivered with PI-10 seconds) during shRNA plasmid-bearing microbubble administration and circulation, leading to reduced efficiency of anti-angiogenic gene therapy.

Transfection assessment by real-time PCR: assessing VEGFR2 mRNA knockdown and green fluorescent protein transfection of remote organs
After UTMD of VEGFR2 shRNA plasmid, VEGFR2 mRNA expression within tumor tissue, as assessed by quantitative real-time PCR, was increasingly reduced as the PI was increased till 10 seconds, with maximum knockdown of VEGFR2 in the tumors treated at PI-10 seconds (**Figure 4**).

a

Progressive tumor replenishment during perfusion imaging

Control

Plasmid IV

Scrambled plasmid

PI-2 s

PI-5 s

PI-10 s

PI-20 s

b

Progressive tumor replenishment during perfusion imaging

Control

Plasmid IV

Scrambled plasmid

PI-2 s

PI-5 s

PI-10 s

PI-20 s
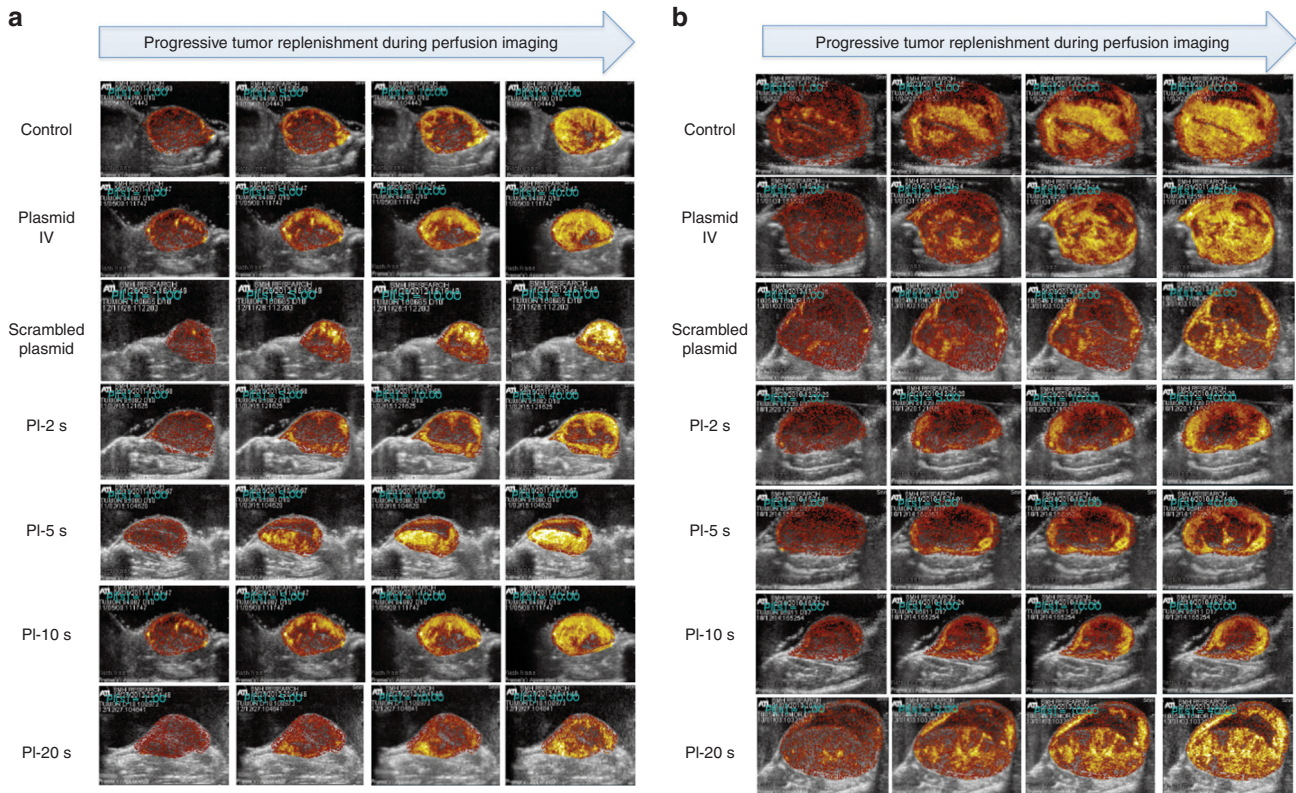
Figure 2 Representative contrast-enhanced ultrasound perfusion images of heterotopic mammary tumors on (a) day 10 (pre-UTMD) and (b) day 17 (7 days after UTMD) at increasing time points (pulsing intervals (PIs) of 1, 5, 10, and 40 seconds) during microbubble replenishment with perfusion imaging, for all treatment groups. Images are color coded, with bright yellow/orange signifying the highest acoustic signal and greatest perfusion. As PIs during anti-VEGFR2 UTMD is increased till PI-10 seconds, tumor size becomes smaller with the largest tumors seen in the control, scrambled, and plasmid IV groups. Visually, tumor perfusion is greater and more complete throughout the tumor in the control and plasmid IV groups, with the most reduced perfusion seen in tumors of the PI-5 seconds– and PI-10 seconds–treated groups. UTMD, Ultrasound-targeted microbubble destruction; VEGFR2, vascular endothelial growth factor receptor-2.

While systemic intravenous injection of VEGFR2 shRNA plasmid led to a marginally reduced mRNA expression of VEGFR2, ultrasound-mediated delivery of microbubbles bearing shRNA plasmid DNA produced greater reductions in VEGFR2 mRNA expression within tumors.

VEGFR2 expression by PCR in remote organs, liver, lung, kidney and spleen showed no significant knockdown of VEGFR2 across all treatment groups (data not shown). Data on green fluorescent protein (GFP) transfection in remote organs are shown in **Figure 5**. Transfection was very low in all organs across treatment groups, with only minimal transfection seen only in the Plasmid IV group in liver, lung, and spleen. Combined together, these data provide evidence of the target specificity of ultrasound-mediated gene delivery.

Western blot analysis: VEGFR2 protein knockdown
Western blot analysis revealed a gradual decrease in VEGFR2 expression at the protein level as the PI during UTMD increased from PI-2 seconds to PI-5 seconds, and then to PI-10 seconds (**Figure 6a**). The relative protein expression as normalized to the internal control was markedly reduced at all PIs as compared with control groups (**Figure 6b**). There was also a significant difference in protein expression levels at PI-10 seconds compared with other PIs.

Immunohistochemistry: VEGFR2
Immunostaining for VEGFR2 expression within tumor vasculature showed a gradual reduction in VEGFR2 expression as the PI during UTMD increased from PI-2 seconds to PI-5 seconds, and then to PI-10 seconds, when compared with tumor treated at PI-20 seconds, non-treated control tumors, tumors treated with intravenous plasmid and tumors treated with scrambled plasmid. Similar to the RT-PCR data and western blot analysis, UTMD of VEGFR2 shRNA plasmid at a PI of 10 seconds resulted in the lowest expression of VEGFR2 (**Figure 7**). These findings suggest the anti-angiogenic effect of ultrasound-mediated shRNA gene therapy is mediated by effective knockdown of VEGFR2, with the greatest effect at the PI of 10 seconds. No adverse effects from ultrasound exposure were detected by histology.

Discussion

In order for small interfering RNA (siRNA)-based gene approaches for cancer treatment to become a clinical reality, gene therapy requires a site-specific, effective, and safe delivery platform.[5] Ultrasound-mediated gene transfection by UTMD meets several of these criteria, making it an attractive technique for anti-cancer gene therapy. The novel findings of
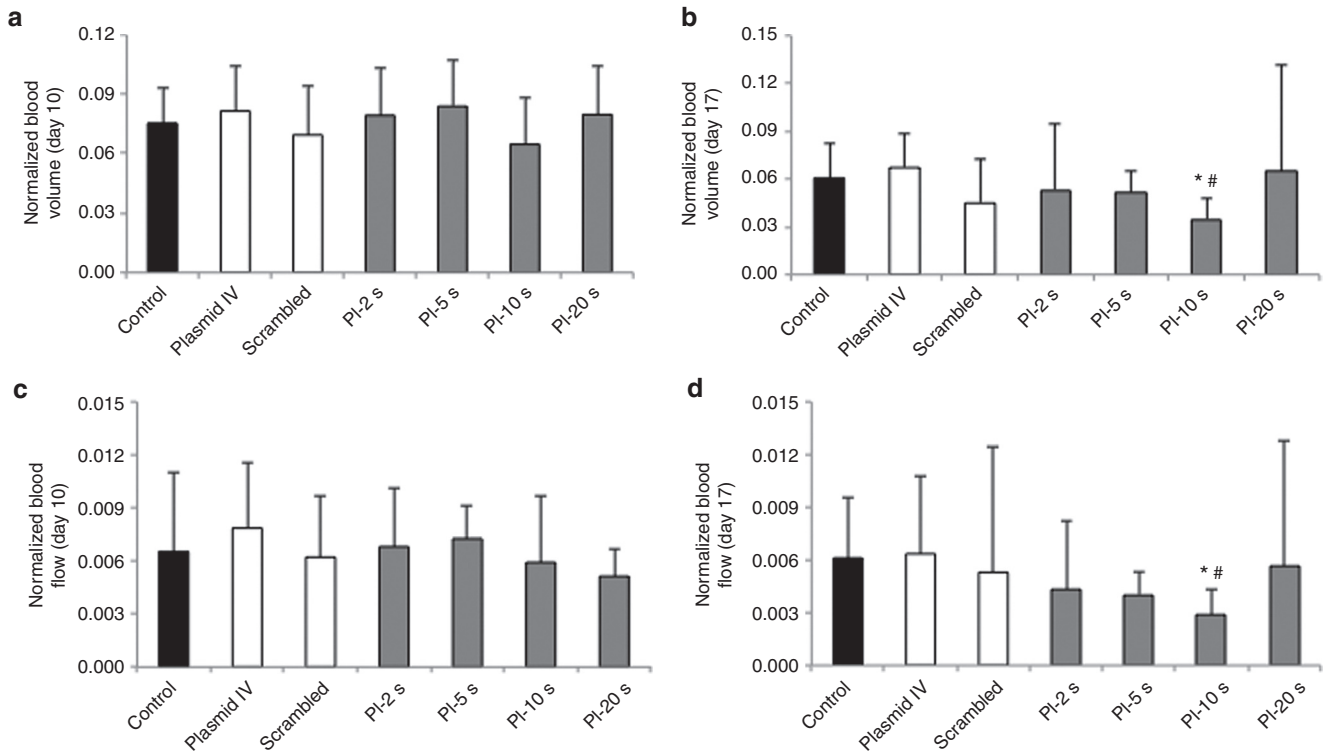
Figure 3 Contrast-enhanced ultrasound tumor perfusion data in all groups. Normalized tumor blood volume at (**a**) day 10 and (**b**) day 17. At day 17, tumor blood volume in PI-10 seconds group was significantly lower compared with control, scrambled, and plasmid IV groups. Normalized tumor blood flow at (**c**) day 10 and (**d**) day 17. At day 17, tumor blood flow was significantly reduced in PI-10 seconds group compared with control groups. $*P < 0.01$ versus control, $\#P < 0.05$ versus plasmid IV and scrambled plasmid. PI, pulsing interval.
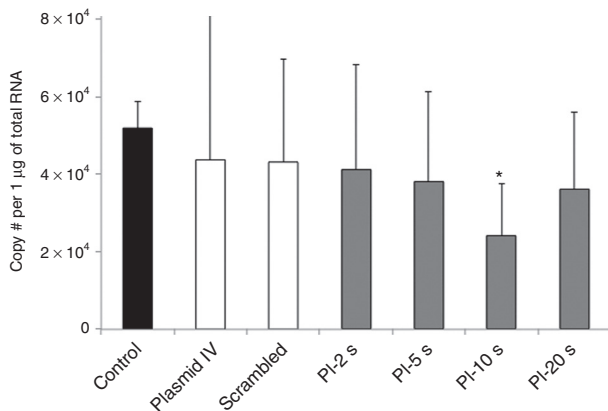
Figure 4 Endogenous VEGFR2 expression in tumor tissue in all treatment groups. There was a significant knockdown of VEGFR2 levels by quantitative PCR in tumors in the PI-10 seconds group, when compared with control, plasmid IV, and scrambled plasmid groups. $*P < 0.05$ versus control, plasmid IV, and scrambled plasmid; #, number. PI, pulsing interval; VEGFR2, vascular endothelial growth factor receptor-2.

our present study are that (i) anti-angiogenic cancer gene therapy using ultrasound-mediated delivery of microbubbles bearing anti-VEGFR2 shRNA plasmid DNA results in targeted knockdown of VEGFR2 within tumors, and subsequently lower tumor microvascular perfusion and attenuated growth, and (ii) longer PIs during UTMD which allow complete replenishment of plasmid-bearing microbubbles into the tumor microvasculature in between high-power destructive delivery pulses produces the greatest target knockdown and anti-tumor effect.

The clinical translation of siRNA-based cancer therapies is limited by several challenges, including (i) short half-life after systemic administration due to clearance by the reticulo-endothelial system[23] and degradation by serum ribonucleases, (ii) poor, transient uptake within tumors due to size and negative charge, and (iii) off-target effects and toxicity.[5] To overcome these hurdles, systemic siRNA administration is often performed using various carriers,[5,6,24] such as nanoparticles[25,26] or liposomes,[27,28] to enhance bioavailability, prolong circulation time and avoid elimination, and to improve uptake to target organs. Similar to nanoparticles and liposomes, gas-filled microbubbles (2–3 μm in diameter) can act as delivery vehicles for plasmid DNA and siRNA, prolonging their bioavailability in circulation. When given intravenously, transfection can be targeted to specific tissues by the focused external application of high-power ultrasound that destroys the microbubble-gene complexes, resulting in transfection of the vascular endothelium and surrounding cells via several mechanisms, including cavitation, microjet formation, and microporation.[29,30] This unique ability to target delivery to the vascular endothelium makes it attractive for pro-angiogenic gene therapy, and as we demonstrate in this study, for anti-angiogenic cancer gene therapy targeted against VEGFR2.

For our present study, we targeted VEGFR2 using shRNA plasmid gene therapy using UTMD to suppress tumor

GFP expression
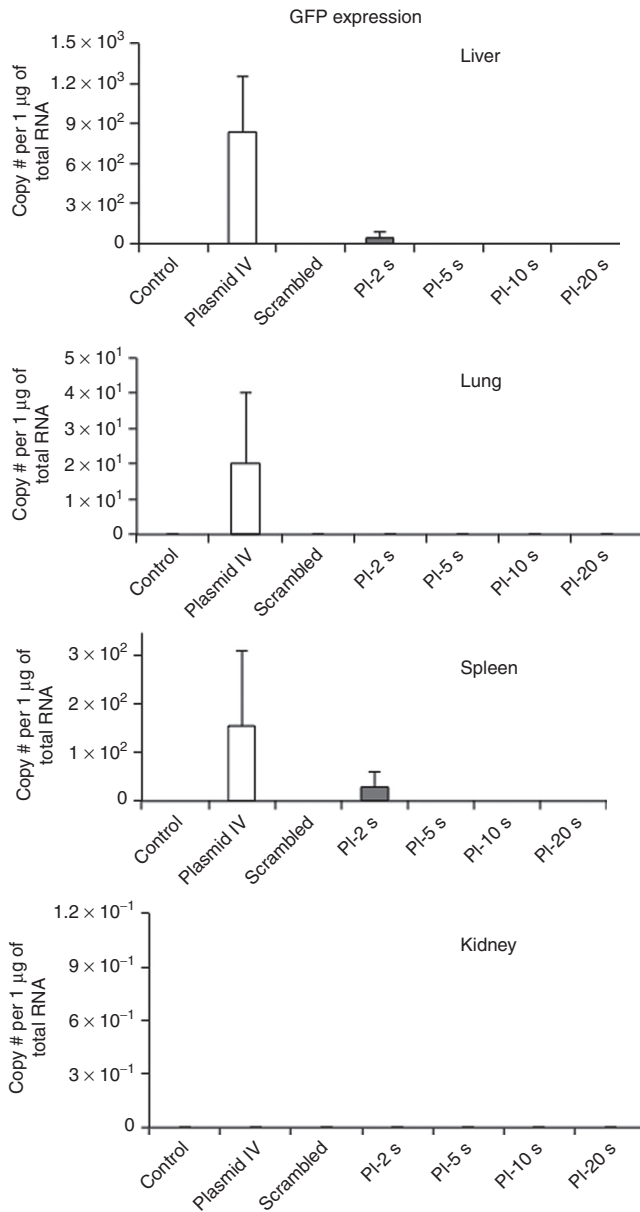
Figure 5 GFP mRNA levels in remote organs, as a measure of off-target transfection. GFP mRNA levels were measured by quantitative real-time PCR in all treatment groups in (**a**) lung, (**b**) spleen, (**c**) liver, and (**d**) kidney. Transfection was very low in all organs across treatment groups, with only minimal transfection seen in the Plasmid IV group in liver, lung, and spleen. PI, pulsing interval. #, number.

a

b

Figure 6 Endogenous VEGFR2 protein expression in tumor tissue for all treatment groups. (**a**) Relative intensity of VEGFR2 protein in all the groups normalized to internal control β-actin levels. VEGFR2 protein levels were reduced in all the treatment groups, with maximal reduction observed at PI-10 seconds. (**b**) Gradual decrease in VEGFR2 protein levels as developed on X-ray film in all treatment groups with no significant reduction in control, scrambled, and plasmid IV groups ($^{\#}P < 0.01$ versus control, plasmid IV, and scrambled). There was a significant difference in protein expression levels at PI-10 seconds compared with other PIs. $*P < 0.05$ versus PI-2 seconds, PI-5 seconds and PI-20 seconds. PI, pulsing interval; VEGFR2, vascular endothelial growth factor receptor-2.

angiogenesis in a heterotopic model of mammary adenocarcinoma. To our knowledge, only two studies have performed *in vivo* studies of UTMD using an anti-angiogenic strategy, both of which used direct injections of microbubbles and DNA as opposed to systemic intravenous injections used in our present study. Duvshani-Eshet *et al.* used UTMD to deliver genes encoding for hemopexin-like domain fragment (PEX), an inhibitor of angiogenesis, to heterotopic prostate tumors in mice.[21] Repeated intra-tumoral injections of PEX plus Optison microbubbles in conjunction with therapeutic ultrasound inhibited prostate tumor growth by 80%, with reduced tumor vascularity. Liao *et al.* performed UTMD of anti-angiogenic genes by direct intramuscular injections into skeletal muscle as adjuvant therapy to treat distant orthotopic tumors in mice.[20] They demonstrated that repeated ultrasound-mediated delivery of endostatin or calreticulin with SonoVue microbubbles by intramuscular injections into hindlimb skeletal muscle significantly inhibited the growth of tumors in liver, brain, or lung.[20]

Recently, Carson *et al.* performed EGFR–directed small inhibitory RNA (siRNA) therapy using UTMD to treat murine squamous cell carcinomas.[31] They demonstrated significant inhibition of tumor growth with this strategy, however, recognized the need for optimization of ultrasound parameters to achieve even higher degrees of tumor growth inhibition. Intravenous siRNA plasmid delivery with UTMD as in our study has certain advantages. First, it allows gene therapy to be non-invasive, where repeated deliveries can be readily performed for more sustained transfection[32] or multiple genes can be delivered to achieve a synergistic therapeutic effect.[12,33] Second, although transfection is lower compared with direct injections, it results in targeted vascular transfection over a wider distribution, and results in a more efficient therapeutic response.[10] Our prior study of pro-angiogenic gene delivery using UTMD have not detected remote transfection in organs outside the ultrasound beam,[9] and similarly our present study findings did not reveal any significant knockdown of VEGFR2 or GFP transfection in remote organs.

An important and novel component of our study was the determination of the optimal PI to use during UTMD for maximal
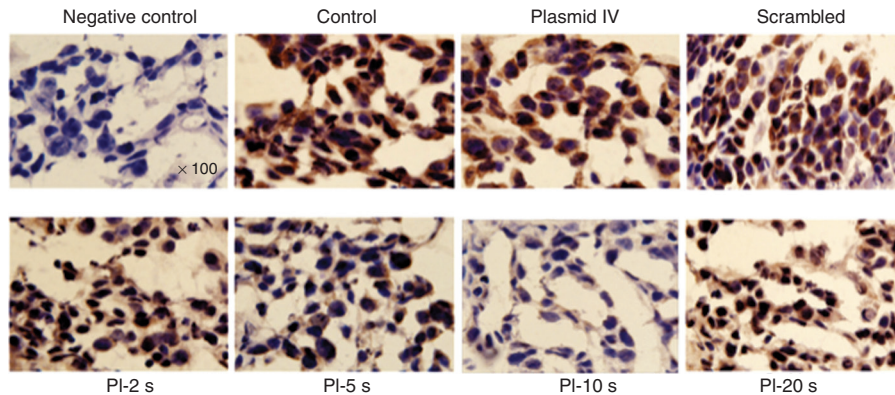
Figure 7 Immunohistochemical staining for VEGFR2 in mammary tumors from all treatment groups. VEGFR2 staining is illustrated by positive brown color and nuclei by purple staining. VEGFR2 staining was reduced in all treatment groups compared with non-treated control, scrambled, and plasmid IV groups, with maximal reduction seen in the PI-10 seconds group. Images taken at original magnification ×100. The primary antibody was omitted in the negative control (upper left panel) to test it's specificity to VEGFR2. PI, pulsing interval; VEGFR2, vascular endothelial growth factor receptor-2.

anti-angiogenic effect. Chen *et al.*[34] investigated the optimal ultrasound settings for UTMD of non-functional reporter genes into the myocardium. They found that transfection was maximized with intermittent ultrasound pulses (every four cardiac cycles) to allow complete filling of the myocardial capillary bed by microbubbles. When continuous ultrasound was used, transfection was significantly reduced due to continual microbubble-gene complex destruction without allowing full replenishment (and hence transfection) into the target tissue. Using our delivery probe (S3), which has a beam thickness of 5 mm at the focal point, we were able to quantify the microbubble replenishment kinetics within our tumors before gene delivery. As expected, the tumor microvasculature was disorganized, and filled slowly. With a mean β value of 0.13, this translates to an average time of 7.7 seconds for full replenishment of the tumor microvasculature at day 10. Thus, during UTMD, a PI-10 seconds allowed complete replenishment of shRNA plasmid-bearing microbubbles in between destructive ultrasound pulses, and was less complete at shorter PIs of 2 and 5 seconds. Given this finding, it is not surprising that maximal reduction in VEGFR2 expression was seen at the PI of 10 seconds. Longer PIs of 20 seconds resulted in reduced efficiency of UTMD despite complete replenishment, likely due to less destructive pulses (half that of PI-10 seconds) during microbubble-gene administration. While tumor volumes were lowest at PI-5 seconds and PI-10 seconds, tumor MBV and flow were most reduced after UTMD at a PI of 10 seconds. Western blot analysis, quantitative PCR and immunostaining confirmed maximal VEGFR2 inhibition at PI-10 seconds, in keeping with data on tumor volume and perfusion parameters. Our findings have important implications for UTMD gene delivery, where assessment of the kinetics of microbubble replenishment in the specific target organ or tumor could be important for optimizing parameters to obtain maximal therapeutic benefit.

Our study has several important limitations. We only followed tumors for 7 days after gene delivery. Given the duration of transfection is limited to 10–14 days,[9,10,32] it is possible that after transfection wanes the tumor may undergo renewed growth. Because of this, future studies will focus on longer time points, repeated deliveries for longer periods of transfection

and knockdown, as well as multigene approaches[12,33] to knockdown targets that have synergistic anti-tumor effects, such as combining anti-angiogenic and pro-apoptotic gene therapies. Our control group that received scrambled plasmid DNA and microbubbles underwent UTMD only at a PI of 10 seconds, as it had the greatest effect with VEGFR2 shRNA plasmid.

In summary, ultrasound-mediated transfection of VEGFR2 shRNA plasmid-bearing microbubbles results in knockdown of VEGFR2, leading to an anti-angiogenic effect and reduced tumor growth. For anti-VEGFR2 gene therapy using UTMD, complete replenishment of tumor vasculature with silencing gene-bearing microbubbles in between destructive pulses is required to maximize the efficacy of anti-angiogenic cancer gene therapy.

Materials and methods

Animal preparation. The study protocol was approved by the Animal Care and Use Committee at the Keenan Research Centre in the Li Ka Shing Knowledge Institute, St Michael's Hospital, University of Toronto. Rats were anesthetized with 2% inhaled isoflurane and maintained in a surgical plane. Under sterile conditions, tumor plugs were created at day 0 by subcutaneous injection of 250,000 rat mammary adeno-carcinoma cells [13762 MAT B III, ATCC Catalog No. CRL-1666] suspended in 250 µl of matrigel. Tumor plugs were injected subcutaneously over the left proximal hindlimb muscle of male Fischer-344 rats (Charles River, Wilmington, MA). For gene delivery and perfusion studies an intravenous catheter was placed in a jugular vein and animals monitored and given analgesia (Anafen 5 mg/kg s.c.) as required.

Microbubble and DNA preparation. For anti-angiogenic gene therapy, cationic lipid-shelled perfluoropropane microbubbles were created by sonicating an aqueous dispersion of 1 mg·ml⁻¹ polyethyleneglycol-40 stearate (Sigma, St Louis, MO), 2 mg·ml⁻¹ distearoyl phophatidylcholine (Avanti, Alabaster, AL) and 0.4 mg·ml⁻¹ 1,2-distearoyl-3-trimethylammoniumpropane (Avanti) with decafluorobutane gas.[10–12] For perfusion imaging, perflutren lipid microspheres (Definity,

Lantheus Medical Imaging, North Billerica, MA) were used. Microbubble concentrations were determined using a Coulter Multisizer IIe (Beckman-Coulter, Brea, CA), before intravenous administration. For gene delivery, cationic lipid microbubbles were charge-coupled to 500 µg of VEGFR2 short hairpin (sh)RNA in plasmid form (Qiagen, Hilden, Germany). Previous studies have shown that this results in ~6,700 plasmids per cationic microbubble.[12] This plasmid also contained the GFP gene under a separate promoter, which allows measurement of GFP mRNA as indirect measure of plasmid expression in remote organs. Plasmids were amplified by One shot Top 10, competent cells (Invitrogen, Carlsbad, CA), purified by EndoFree Plasmid Giga Kits (Qiagen), and diluted with saline to a final concentration of 1 µg/µl.

CEU perfusion imaging. CEU perfusion imaging of tumors was performed using pulse inversion Doppler imaging (L7-4 transducer, HDI 5000; Philips Ultrasound, Andover, MA) at a mechanical index of 1.0 and a transmit frequency of 3.3 MHz during intravenous infusion of lipid microbubbles (Definity).[11,12] The transducer was over the center of the tumor and fixed in position during CEU imaging. Background images were acquired before microbubble infusion. Blood pool signal was measured from a region of interest placed in the left ventricular (LV) cavity (A_{LV}) at end-diastole during a microbubble intravenous infusion rate of 1/10th used for perfusion imaging (1×10^6 min^{-1}) to avoid dynamic range saturation when normalizing tumor plateau acoustic signal for microbubble concentration. Inter animal microbubble concentration in the LV cavity varied by ~16%. The microbubble infusion rate was then increased to 1×10^7 min^{-1} and intermittent imaging was performed by gradually increasing the PI, specifically 0.2, 0.5, 1, 2, 3, 5, 7, 10, 20, and 40 seconds, using an internal timer. The averaged background frames were digitally subtracted from the averaged contrast-enhanced frames at each PI. Regions of interest were drawn encompassing the entire tumor. The PI versus signal intensity data were fit to the function, $y = A (1 - e^{-\beta t})$, where y is signal intensity at the PI t, the A is the plateau signal intensity reflecting MBV, and the β is the rate constant reflecting microbubble or red cell velocity.[35] Normalized MBV was calculated as $A/(A_{LV} \times 10)$. Normalized microvascular blood flow was calculated as $[A/(A_{LV} \times 10)] \times \beta$.

For determination of microbubble replenishment characteristics in untreated tumors (at day 10) with the UTMD delivery probe, CEU tumor perfusion imaging was performed in a subset of animals ($n = 12$) using the S3 transducer (Sonos 5500; Philips Ultrasound) at settings similar to UTMD delivery, and analyzed for β, the rate constant reflecting microbubble velocity within tumors.

Ultrasound-mediated gene delivery. For UTMD, ultrasound was transmitted using a phased array transducer (S3, Sonos 5500; Philips Ultrasound) at 1.3 MHz and a transmit power of 0.9 W (120 V, 9 mA),[9,11] at various PIs: 2, 5, 10, and 20 seconds. In our prior study, using these settings, peak negative acoustic pressure by needle hydrophone was measured at −2,100 kPa by (assuming a tissue attenuation coefficient of 0.3 dB/cm/MHz, at tissue depth of 1 cm).[10] Cationic microbubbles (1×10^9) coupled with 500 µg of plasmid DNA were infused over 10 minutes intravenously. Ultrasound was applied along the entire area of the tumor, for a total of 20 minutes, until all circulating

microbubble-DNA complexes were destroyed. Control animals received no treatment, plasmid IV animals received only shRNA plasmid injection with no ultrasound administration and scrambled plasmid animals received scrambled plasmid DNA coupled with microbubbles and ultrasound at PI of 10 seconds.

Evaluation of tumor size. Tumor size was evaluated by two methods. The two-dimensional CEU images were taken at a PI of 40 seconds, representing maximum MBV, and used to quantify tumor perfused area and total tumor area. After resection on day 17, tumor volume was measured by volumetric displacement.

Transfection assessment by real-time PCR. The knock-down efficiency of the VEGFR2 shRNA plasmid gene delivery and off-target GFP transfection of remote organs was evaluated by real time PCR. Tissue was homogenized in Trizol (Invitrogen) and phase-separated with chloroform according to manufacturer's protocol. This lysate was then purified with a Bio-Rad Aurum Total RNA Mini Kit (Bio-Rad, Mississauga, Ontario, Canada). Quantitative real-time PCR was performed using iScript cDNA Synthesis Kit and SYBR Green (Bio-Rad) following manufacturer's protocols. Standard curves were constructed based on the serial dilution of VEGFR2 (standard) purified from PCR reactions using the PCR purification kit (Invitrogen) and on the serial dilution of GFP-shRNA plasmid (standard) containing the target sequence (GFP). The CT values of the diluted standard VEGFR2 were read out, and plotted versus the logarithm of the number of template copies. The data were fitted to the equation: $Y = k * \log(x) + Y_{intercept}$ where, Y is the Ct value, x is the initial copy number, k is the slope of the curve. Analyzed data was then presented as number of mRNA copies per one µg of total RNA. Specific gene primers and respective annealing temperatures were applied [VEGFR2 primers: <forward 5-GCTCCTGCAGTGCATAACCTGG-3; reverse 5-CTTAGATAGCCCGGAACGCTAC-3> at 60 °C, GFP: <forward 5-AGCCCGACATGAAGATCAAG-3; reverse 5-GGGATGTCCTTGGGGTACTT-3> at 60 °C, and rat cyclophilin primers: <forward 5-ACCCCACCGTGTTCTTCGAC-3; reverse 5-CATTTGCCATGGACAAGATG-3> at 60 °C]. Cyclophilin was used as the housekeeping gene.

Immunohistochemistry. Isolated tissue was cut in cross-section, embedded in O.C.T. compound (Tissue-Tek, Fisher Scientific, Pittsburgh, PA) in large cryomolds, and stored at −80 °C. Frozen tissue blocks were processed and cut into 10 µm-thick sections and fixed immediately with 2% paraformaldehyde. Cryosections were blocked first with 3% H_2O_2 for 1 hour, then 30 minutes of normal goat serum. A primary antibody, rabbit polyclonal to VEGFR2 (Abcam, Toronto, Ontario, Canada) was added at 1:100 dilution and incubated overnight at 4 °C. The secondary antibody, goat polyclonal to rabbit IgG conjugated with HRP (Abcam Invitrogen, Eugene, OR), was added for 1 h at room temperature at a dilution of 1:500, followed by 15 minutes of DAB (Molecular Probes Invitrogen, Eugene, OR) color development. Tissues were counterstained with Mayer's Hematoxylin (Sigma) for 3 min and mounted with CC/Mount (Sigma), followed by heating at 70 °C for 15 min. For oil lens visualization, an organic based mounting medium, Permount, was used. Images were taken with Olympus BX50 at 100× magnification (Olympus, Center Valley, PA).

Western blotting. Isolated tissue was cut into appropriate sections and lysed in RIPA buffer (Sigma) by sonication. The protein concentrations were determined by Bradford Assay (Bio-Rad) and 80 µg of protein was loaded in each well. The gel was allowed to run at 100 V till it reached resolving gel and was adjusted to 120 V for the rest of the process. Transfer was performed at 80 V at room temperature for 2–3 hours. After transfer, the membrane was stained with Ponceau Red for less than a minute to detect bands and confirm the transfer. The membrane was then kept in blocking buffer for 1 hour under shaking conditions. The membrane was then rinsed with washing buffer and primary antibodies were added (anti-VEGFR2 at 1:1,000, Abcam; anti-β-actin at 1:5,000, Abcam) and incubated overnight at 4 °C. The membrane was rinsed again and anti Rabbit HRP secondary antibody (1:5,000, Promega, San Luis Obispo, CA) was added to detect VEGFR2 and anti mouse HRP secondary antibody (1:5,000, Promega) to detect β-actin. The membrane was incubated with secondary antibodies for 45 minutes under shaking conditions. After final washes, the blot was developed with ECL detection kit (Amersham, GE Healthcare, Baie-d'Urfé, Quebec, Canada) on a photo film (Kodak, Sigma). Densitometric readings were obtained using the Quantity One software (Bio-Rad) and the sample protein concentrations were normalized to the intensity of β-actin. Western blotting analysis was performed on a total of 42 samples, $n = 6$ for each group.

Experimental protocol. A total of 110 rats underwent tumor plug implantation. CEU perfusion imaging of the tumors was performed at day 10 and day 17 after implantation. Immediately post CEU perfusion (day 10), UTMD gene delivery was performed, according to assigned treatment groups: PI-2 seconds: PI of 2 seconds with 500 µg VEGFR2 shRNA plasmid ($n = 16$); PI-5 seconds: PI of 5 seconds with 500 µg VEGFR2 shRNA plasmid ($n = 16$); PI-10 seconds: PI of 10 seconds with 500 µg VEGFR2 shRNA ($n = 15$); PI-20 seconds: PI of 20 seconds with 500 µg VEGFR2 shRNA ($n = 15$), scrambled DNA-PI of 10 seconds with 500 µg scrambled plasmid ($n = 15$); plasmid IV – Intravenous injection of 500 µg VEGFR2 shRNA with no microbubbles or ultrasound ($n = 15$); control: no treatment ($n = 18$). Tumors were removed for immunohistochemistry, western blotting and RT-PCR at day 17. Remote tissue from liver, lung, kidney, and spleen were also removed for post-mortem analysis.

Statistical analysis. Data are expressed as mean ± SD. Analyses were performed using GraphPad PRISM software (version 5.0a; GraphPad Software, San Diego, CA). Comparisons between treatment groups were performed using one-way ANOVA followed by Tukey's post-test. *P* values <0.05 were considered statistically significant.

1. Rissanen, TT and Ylä-Herttuala, S (2007). Current status of cardiovascular gene therapy. *Mol Ther* **15**: 1233–1247.
2. Zhang, Y and Friedlander, RM (2011). Using non-coding small RNAs to develop therapies for Huntington's disease. *Gene Ther* **18**: 1139–1149.
3. Gardlik, R, Behuliak, M, Palffy, R, Celec, P and Li, CJ (2011). Gene therapy for cancer: bacteria-mediated anti-angiogenesis therapy. *Gene Ther* **18**: 425–431.
4. Schenk, E, Essand, M, Bangma, CH, Barber, C, Behr, JP, Briggs, S *et al.*; GIANT FP6 Consortium. (2010). Clinical adenoviral gene therapy for prostate cancer. *Hum Gene Ther* **21**: 807–813.
5. Rettig, GR and Behlke, MA (2012). Progress toward in vivo use of siRNAs-II. *Mol Ther* **20**: 483–512.
6. Järver, P, Coursindel, T, Andaloussi, SE, Godfrey, C, Wood, MJ and Gait, MJ (2012). Peptide-mediated Cell and In Vivo Delivery of Antisense Oligonucleotides and siRNA. *Mol Ther Nucleic Acids* **1**: e27.
7. Zhang, Y, Satterlee, A and Huang, L (2012). In vivo gene delivery by nonviral vectors: overcoming hurdles? *Mol Ther* **20**: 1298–1304.
8. Smith, AH, Fujii, H, Kuliszewski, MA and Leong-Poi, H (2011). Contrast ultrasound and targeted microbubbles: diagnostic and therapeutic applications for angiogenesis. *J Cardiovasc Transl Res* **4**: 404–415.
9. Leong-Poi, H, Kuliszewski, MA, Lekas, M, Sibbald, M, Teichert-Kuliszewska, K, Klibanov, AL *et al.* (2007). Therapeutic arteriogenesis by ultrasound-mediated VEGF165 plasmid gene delivery to chronically ischemic skeletal muscle. *Circ Res* **101**: 295–303.
10. Kobulnik, J, Kuliszewski, MA, Stewart, DJ, Lindner, JR and Leong-Poi, H (2009). Comparison of gene delivery techniques for therapeutic angiogenesis ultrasound-mediated destruction of carrier microbubbles versus direct intramuscular injection. *J Am Coll Cardiol* **54**: 1735–1742.
11. Kuliszewski, MA, Kobulnik, J, Lindner, JR, Stewart, DJ and Leong-Poi, H (2011). Vascular gene transfer of SDF-1 promotes endothelial progenitor cell engraftment and enhances angiogenesis in ischemic muscle. *Mol Ther* **19**: 895–902.
12. Smith, AH, Kuliszewski, MA, Liao, C, Rudenko, D, Stewart, DJ and Leong-Poi, H (2012). Sustained improvement in perfusion and flow reserve after temporally separated delivery of vascular endothelial growth factor and angiopoietin-1 plasmid deoxyribonucleic acid. *J Am Coll Cardiol* **59**: 1320–1328.
13. Nie, F, Xu, HX, Lu, MD, Wang, Y and Tang, Q (2008). Anti-angiogenic gene therapy for hepatocellular carcinoma mediated by microbubble-enhanced ultrasound exposure: an in vivo experimental study. *J Drug Target* **16**: 389–395.
14. Carson, AR, McTiernan, CF, Lavery, L, Hodnick, A, Grata, M, Leng, X *et al.* (2011). Gene therapy of carcinoma using ultrasound-targeted microbubble destruction. *Ultrasound Med Biol* **37**: 393–402.
15. Zhou, S, Li, S, Liu, Z, Tang, Y, Wang, Z, Gong, J *et al.* (2010). Ultrasound-targeted microbubble destruction mediated herpes simplex virus-thymidine kinase gene treats hepatoma in mice. *J Exp Clin Cancer Res* **29**: 170.
16. Aoi, A, Watanabe, Y, Mori, S, Takahashi, M, Vassaux, G and Kodama, T (2008). Herpes simplex virus thymidine kinase-mediated suicide gene therapy using nano/microbubbles and ultrasound. *Ultrasound Med Biol* **34**: 425–434.
17. Haag, P, Frauscher, F, Gradl, J, Seitz, A, Schäfer, G, Lindner, JR *et al.* (2006). Microbubble-enhanced ultrasound to deliver an antisense oligodeoxynucleotide targeting the human androgen receptor into prostate tumours. *J Steroid Biochem Mol Biol* **102**: 103–113.
18. Chen, ZY, Liang, K, Xie, MX, Wang, XF, Lü, Q and Zhang, J (2009). Induced apoptosis with ultrasound-mediated microbubble destruction and shRNA targeting survivin in transplanted tumors. *Adv Ther* **26**: 99–106.
19. Greco, A, Di Benedetto, A, Howard, CM, Kelly, S, Nande, R, Dementieva, Y *et al.* (2010). Eradication of therapy-resistant human prostate tumors using an ultrasound-guided site-specific cancer terminator virus delivery approach. *Mol Ther* **18**: 295–306.
20. Liao, ZK, Tsai, KC, Wang, HT, Tseng, SH, Deng, WP, Chen, WS *et al.* (2012). Sonoporation-mediated anti-angiogenic gene transfer into muscle effectively regresses distant orthotopic tumors. *Cancer Gene Ther* **19**: 171–180.
21. Duvshani-Eshet, M, Benny, O, Morgenstern, A and Machluf, M (2007). Therapeutic ultrasound facilitates antiangiogenic gene delivery and inhibits prostate tumor growth. *Mol Cancer Ther* **6**: 2371–2382.
22. Rao, DD, Vorhies, JS, Senzer, N and Nemunaitis, J (2009). siRNA vs. shRNA: similarities and differences. *Adv Drug Deliv Rev* **61**: 746–759.
23. Huang, Y, Hong, J, Zheng, S, Ding, Y, Guo, S, Zhang, H *et al.* (2011). Elimination pathways of systemically delivered siRNA. *Mol Ther* **19**: 381–385.
24. Kanasty, RL, Whitehead, KA, Vegas, AJ and Anderson, DG (2012). Action and reaction: the biological response to siRNA and its delivery vehicles. *Mol Ther* **20**: 513–524.
25. Gao, S, Dagnaes-Hansen, F, Nielsen, EJ, Wengel, J, Besenbacher, F, Howard, KA *et al.* (2009). The effect of chemical modification and nanoparticle formulation on stability and biodistribution of siRNA in mice. *Mol Ther* **17**: 1225–1233.
26. Belliveau, NM, Huft, J, Lin, PJ, Chen, S, Leung, AK, Leaver, TJ *et al.* (2012). Microfluidic Synthesis of Highly Potent Limit-size Lipid Nanoparticles for In Vivo Delivery of siRNA. *Mol Ther Nucleic Acids* **1**: e37.
27. Nakayama, T, Butler, JS, Sehgal, A, Severgnini, M, Racie, T, Sharman, J *et al.* (2012). Harnessing a physiologic mechanism for siRNA delivery with mimetic lipoprotein particles. *Mol Ther* **20**: 1582–1589.

28. Wu, SY, Singhania, A, Burgess, M, Putral, LN, Kirkpatrick, C, Davies, NM *et al.* (2011). Systemic delivery of E6/7 siRNA using novel lipidic particles and its application with cisplatin in cervical cancer mouse models. *Gene Ther* **18**: 14–22.

29. Christiansen, JP, French, BA, Klibanov, AL, Kaul, S and Lindner, JR (2003). Targeted tissue transfection with ultrasound destruction of plasmid-bearing cationic microbubbles. *Ultrasound Med Biol* **29**: 1759–1767.

30. Kodama, T, Tomita, Y, Koshiyama, K and Blomley, MJ (2006). Transfection effect of microbubbles on cells in superposed ultrasound waves and behavior of cavitation bubble. *Ultrasound Med Biol* **32**: 905–914.

31. Carson, AR, McTiernan, CF, Lavery, L, Grata, M, Leng, X, Wang, J *et al.* (2012). Ultrasound-targeted microbubble destruction to deliver siRNA cancer therapy. *Cancer Res* **72**: 6191–6199.

32. Bekeredjian, R, Chen, S, Frenkel, PA, Grayburn, PA and Shohet, RV (2003). Ultrasound-targeted microbubble destruction can repeatedly direct highly specific plasmid expression to the heart. *Circulation* **108**: 1022–1026.

33. Fujii, H, Sun, Z, Li, SH, Wu, J, Fazel, S, Weisel, RD *et al.* (2009). Ultrasound-targeted gene delivery induces angiogenesis after a myocardial infarction in mice. *JACC Cardiovasc Imaging* **2**: 869–879.

34. Chen, S, Shohet, RV, Bekeredjian, R, Frenkel, P and Grayburn, PA (2003). Optimization of ultrasound parameters for cardiac gene delivery of adenoviral or plasmid deoxyribonucleic acid by ultrasound-targeted microbubble destruction. *J Am Coll Cardiol* **42**: 301–308.

35. Wei, K, Jayaweera, AR, Firoozan, S, Linka, A, Skyba, DM and Kaul, S (1998). Quantification of myocardial blood flow with ultrasound-induced destruction of microbubbles administered as a constant venous infusion. *Circulation* **97**: 473–483.